

# Computational Neuroscience (EC60007)

## Project II

### Morris-Lecar & Hodgkin-Huxley Models

Roll No: 22CS30053

## 1 Morris-Lecar Model Analysis

### 1.1 Question 1: Consistent Units

Units: ms,  $\mu\text{A}/\text{cm}^2$ , mV,  $\mu\text{F}/\text{cm}^2$ ,  $\text{mS}/\text{cm}^2$ . Verified consistent via Ohm's law:  $[\mu\text{A}/\text{cm}^2] = [\text{mS}/\text{cm}^2] \times [\text{mV}] = 10^{-6} \text{ A}/\text{cm}^2$ . For  $\mu\text{S}/\text{cm}^2$  conductance, use  $\text{pA}/\text{cm}^2$  current (solution not unique).

### 1.2 Question 2: Equilibrium Point and Phase Plane Analysis

Two methods: (1) Nullcline intersection (graphical), (2) Numerical root finding. Equilibrium found at intersection of V-nullcline and w-nullcline.

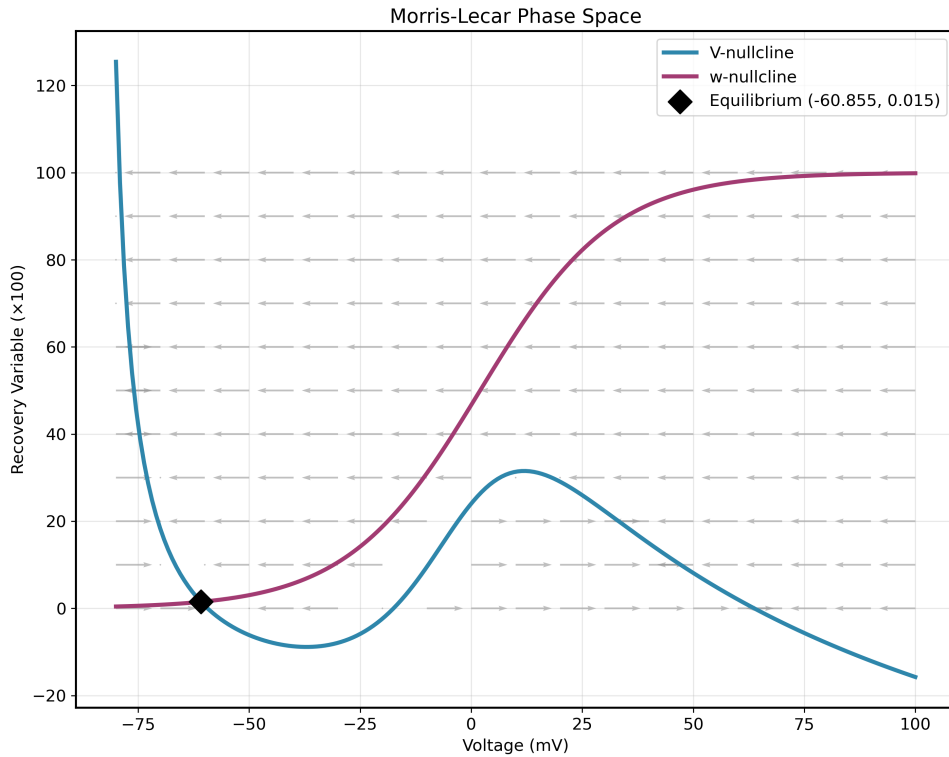


Figure 1: Phase plane with nullclines, equilibrium point, and direction field.

### 1.3 Question 3: Stability Analysis

Stability determined by computing eigenvalues of Jacobian matrix at equilibrium. Equilibrium is stable if all eigenvalues have negative real parts.

## 1.4 Question 4: Numerical Tolerance

Default tolerances ( $\text{AbsTol}=10^{-6}$ ,  $\text{RelTol}=10^{-3}$ ) are reasonable since voltage is  $O(10\text{-}100)$  mV. If voltage in kV, need  $\text{AbsTol} = 10^{-6}$  to  $10^{-5}$  for same absolute accuracy.

## 1.5 Question 5: Action Potentials with Different $\phi$ Values

Parameter  $\phi$  controls recovery timescale. Smaller  $\phi$  (0.01) gives broader action potentials; larger  $\phi$  (0.04) gives narrower, faster recovery.

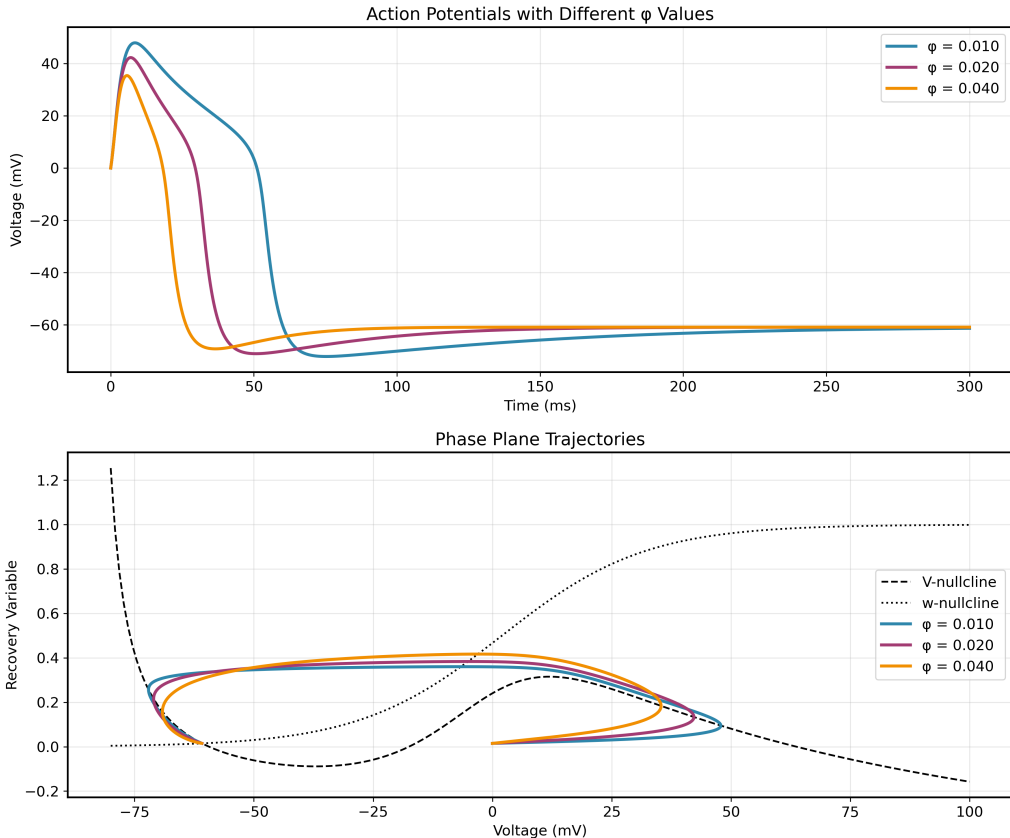


Figure 2: Action potentials for  $\phi = 0.01, 0.02, 0.04$  showing effect on shape and recovery.

## 1.6 Question 6: Depolarization Threshold

Threshold defined as minimum initial depolarization to trigger action potential. MLE exhibits sharp threshold behavior with clear transition from subthreshold to suprathreshold responses.

## 1.7 Question 7: High Current Response

With  $I_{\text{ext}} = 86 \mu\text{A}/\text{cm}^2$ , equilibrium shifts. Different initial conditions (zero-current equilibrium vs high-current equilibrium) lead to different trajectories.

## 1.8 Question 8: Multiple Current Values

System behavior analyzed across multiple currents showing how equilibrium points and stability change with current injection.

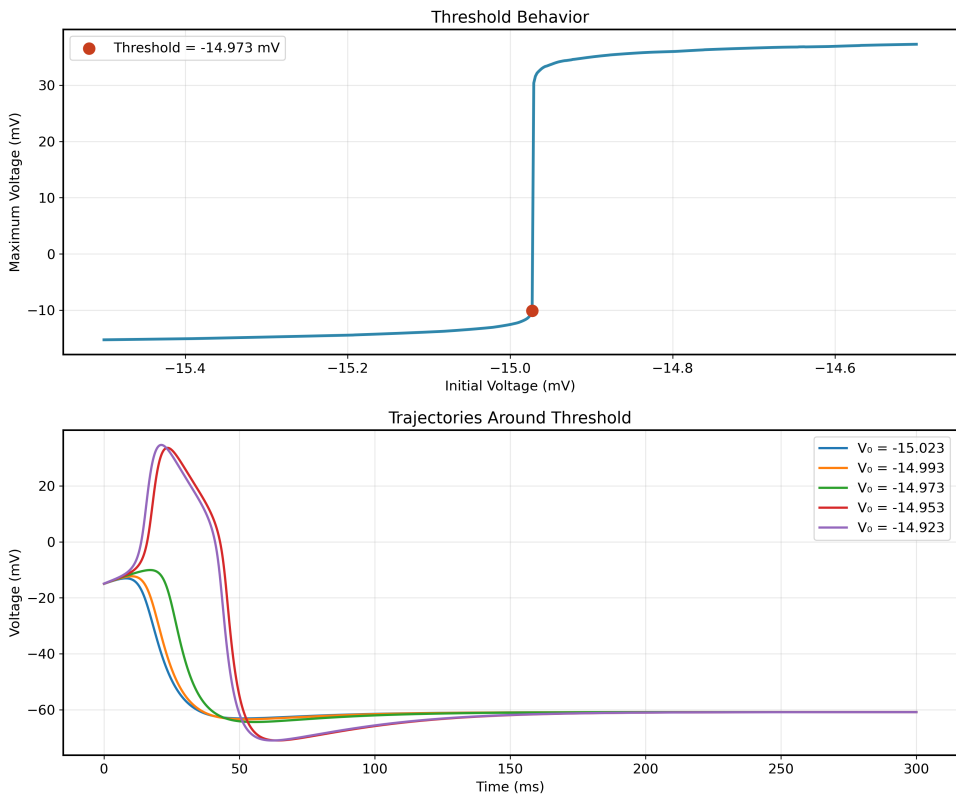


Figure 3: Maximum voltage vs initial depolarization showing threshold.

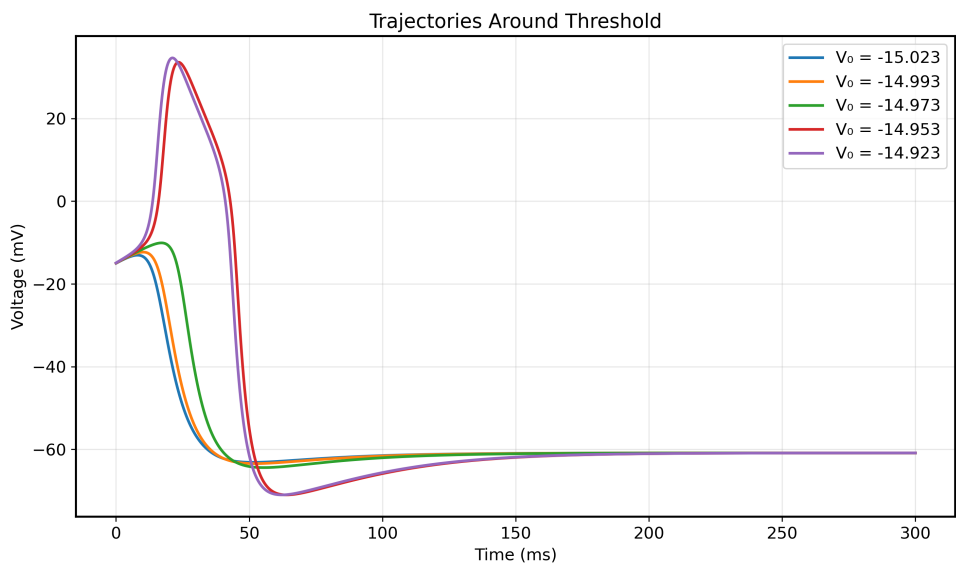


Figure 4: Trajectories around threshold: some produce action potentials, others do not.

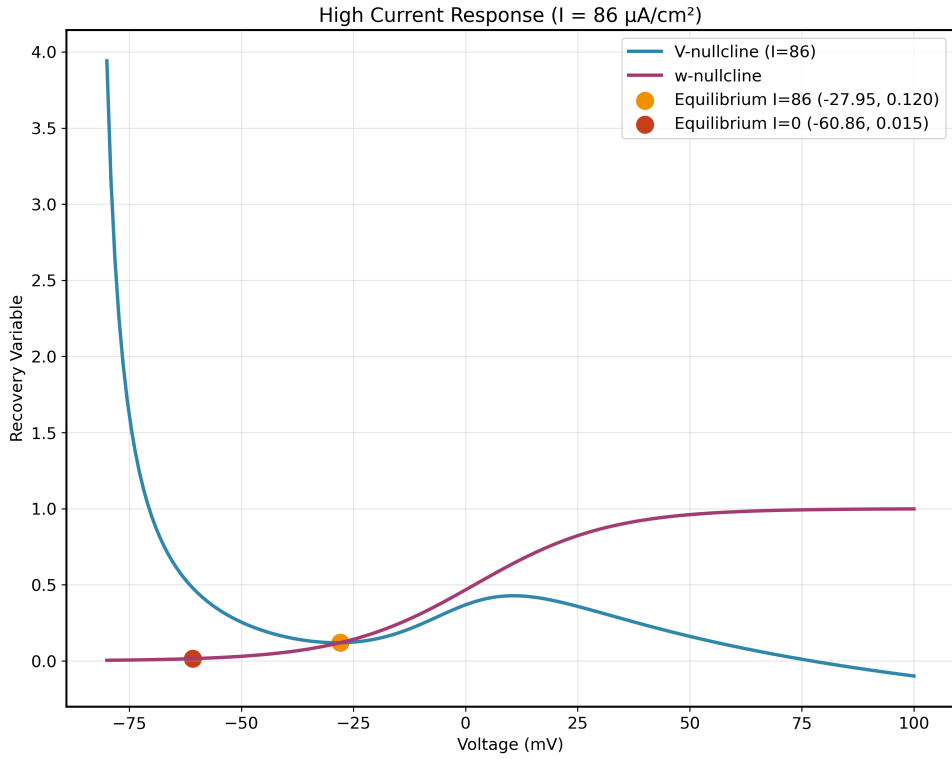


Figure 5: Phase plane at  $I = 86 \mu\text{A}/\text{cm}^2$  showing shifted equilibrium.

### 1.9 Question 9: Firing Rate Analysis

Firing rate increases with applied current in the range  $30\text{-}45 \mu\text{A}/\text{cm}^2$ , demonstrating regular spiking behavior.

### 1.10 Question 10-11: Alternative Parameter Set

With alternative parameters ( $g_{\text{Ca}} = 4$ ,  $V_3 = 12$ ,  $V_4 = 17.4$ ,  $\phi = 0.0667$ ) and  $I_{\text{ext}} = 30 \mu\text{A}/\text{cm}^2$ , system exhibits multiple equilibrium points (typically 3). Between  $39\text{-}40 \mu\text{A}/\text{cm}^2$ , bifurcations occur as equilibrium points change stability.

## 2 Hodgkin-Huxley Model Analysis

### 2.1 Question 12: Model Implementation

HH equations implemented with  $\bar{g}_{\text{Na}} = 120$ ,  $\bar{g}_K = 36$ ,  $\bar{g}_L = 0.3 \text{ mS}/\text{cm}^2$ ,  $C = 1 \mu\text{F}/\text{cm}^2$ . Rate constants  $\alpha_n$  and  $\alpha_m$  handled at  $V = -50$  and  $-35 \text{ mV}$  to avoid  $0/0$  singularities using L'Hôpital's rule limits.

### 2.2 Question 13: Resting Potential Calibration

Leak reversal potential  $E_L$  calibrated to achieve resting potential of  $-60 \text{ mV}$  by solving equilibrium condition. Model produces action potentials with  $I_{\text{ext}} = 10 \mu\text{A}/\text{cm}^2$ .

### 2.3 Question 14: Resting Stability and Threshold

Resting state stability analyzed via Jacobian eigenvalues. Threshold for brief current pulses determined by testing depolarizations of various magnitudes.

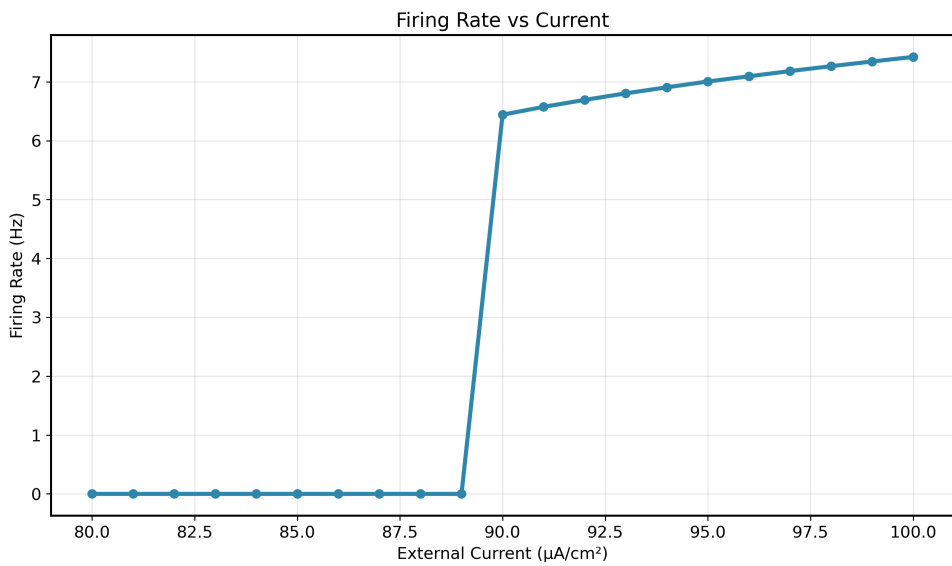


Figure 6: Firing rate vs applied current showing response to increasing stimulation.

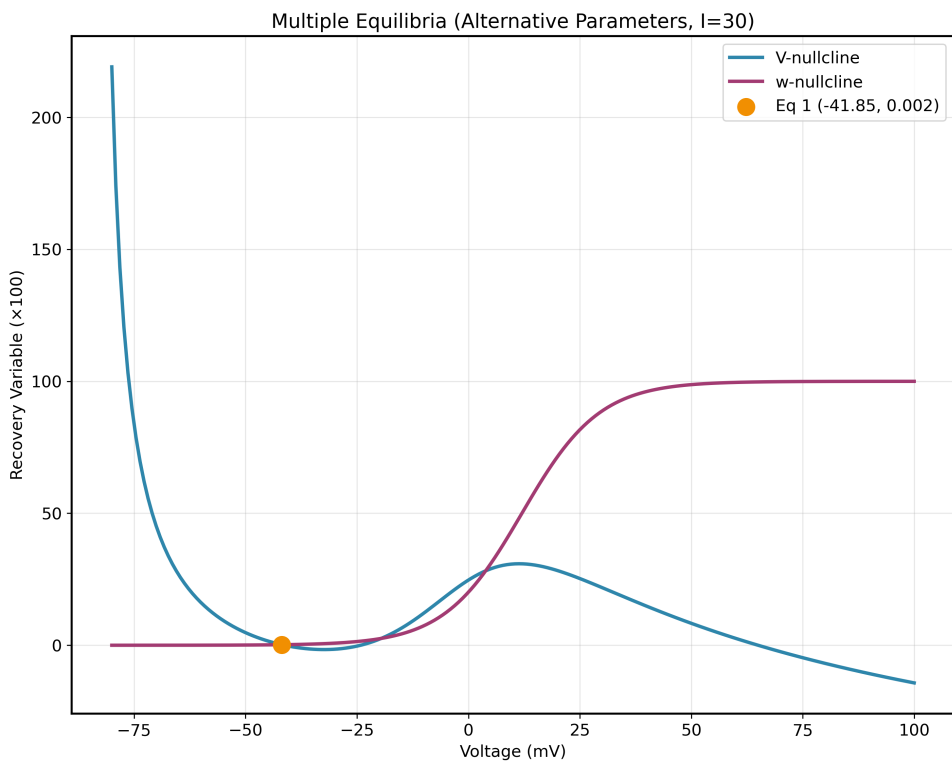


Figure 7: Phase plane showing multiple equilibrium points and their stability.

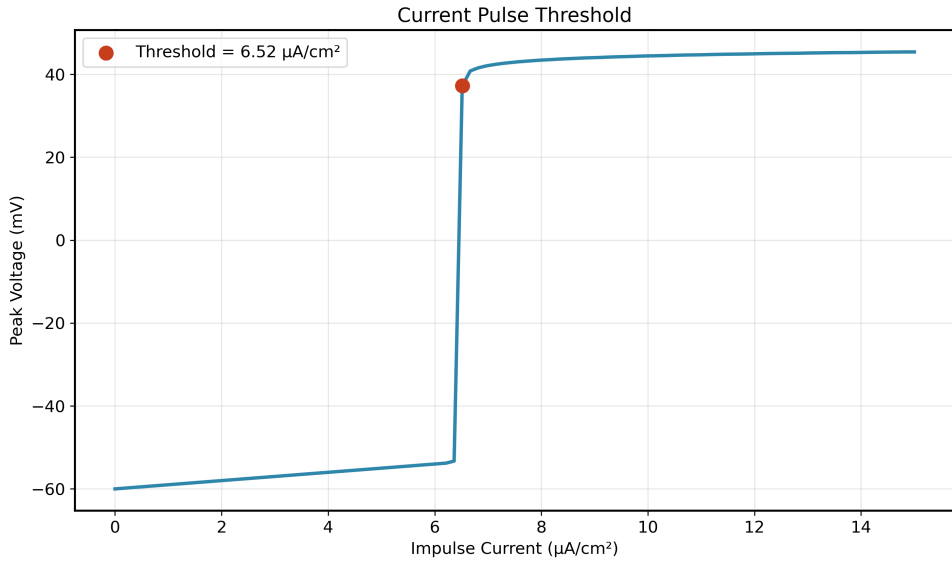


Figure 8: Current pulse threshold analysis.

## 2.4 Question 15: Steady Current Analysis

At  $I = 9 \mu\text{A}/\text{cm}^2$ , equilibrium is stable when computed directly, but starting from zero-current equilibrium leads to limit cycle, demonstrating importance of computing equilibria at each current value.

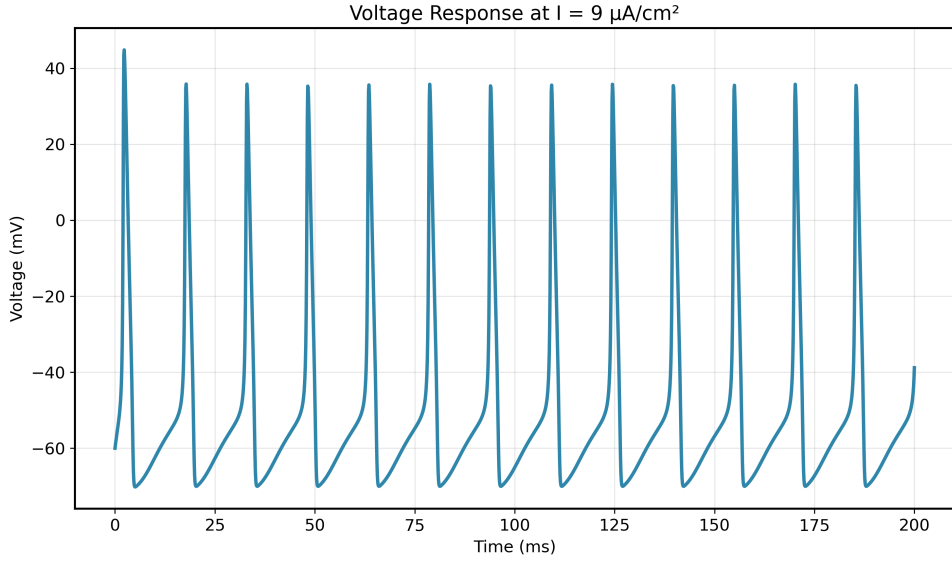


Figure 9: Voltage response at  $I = 9 \mu\text{A}/\text{cm}^2$  showing limit cycle from zero-current initial conditions.

## 2.5 Question 16: Reduced Model

Reduced to two variables ( $V, n$ ) by setting  $m$  and  $h$  to steady-state values. Captures essential dynamics with slight differences in timing and shape.

## 2.6 Question 17: Anode Break Excitation

Hyperpolarizing current ( $-3 \mu\text{A}/\text{cm}^2$  for 20 ms) causes  $h$  to increase and  $n$  to decrease. Upon removal, high  $h$  and low  $n$  create window for sodium dominance, generating action potential.

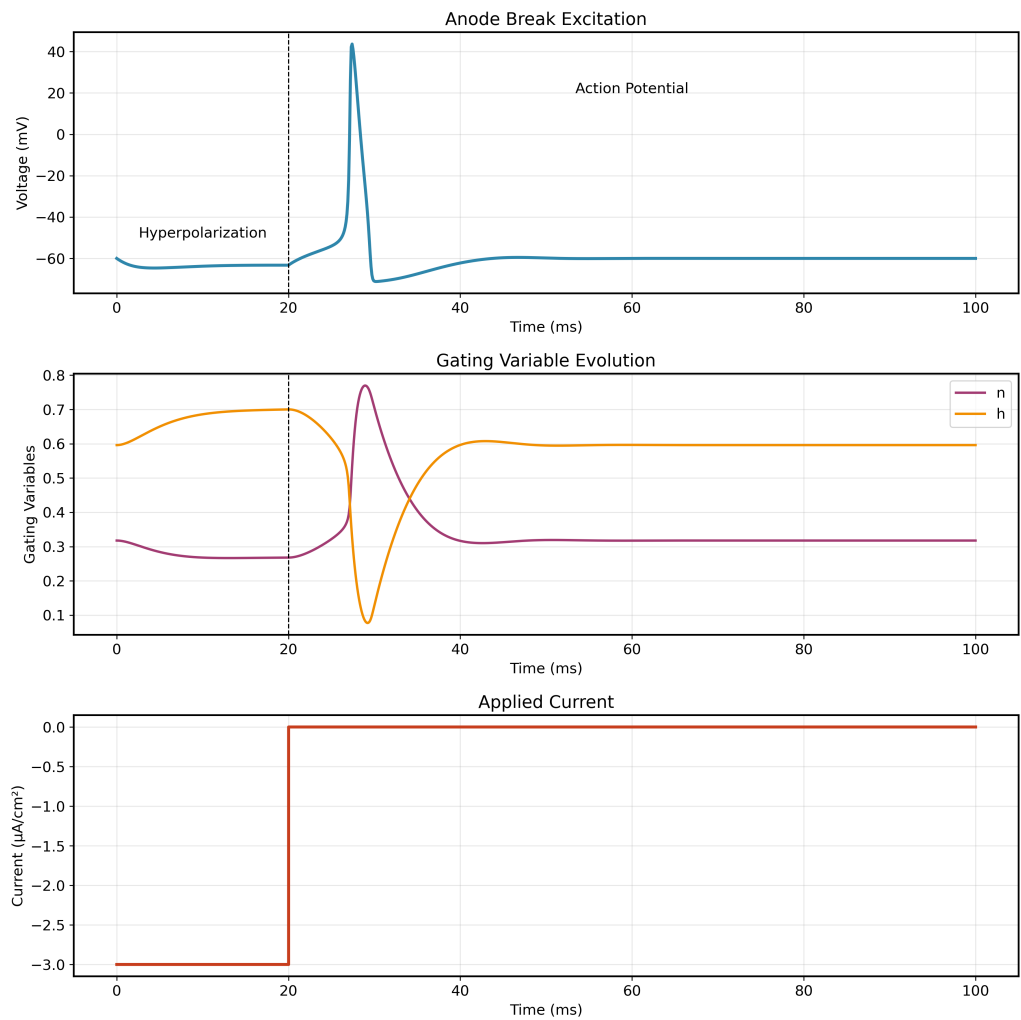


Figure 10: Anode break excitation: action potential after hyperpolarization termination.

## 2.7 Question 18: Reduced Model Phase Plane Analysis

$V - m$  phase plane analyzed with  $n$  and  $h$  fixed at: (1) resting values, (2) post-hyperpolarization values. Case 1 shows stable equilibrium near rest; Case 2 shows unstable/missing equilibrium, explaining anode break excitation.

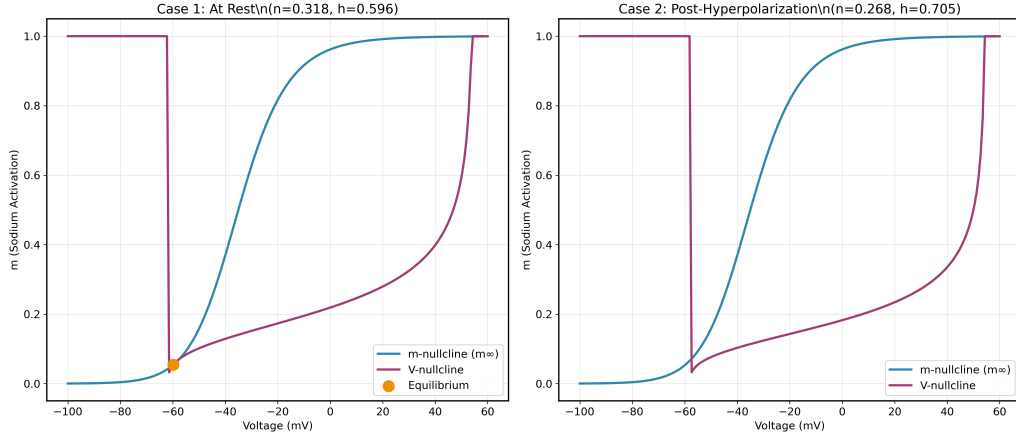


Figure 11:  $V - m$  phase plane: Case 1 (rest) has stable equilibrium; Case 2 (post-hyperpolarization) lacks stable rest point.

## 3 Conclusions

Both models successfully demonstrate key neural phenomena: unit consistency for numerical stability, phase plane analysis insights, threshold behavior, reduced model utility, and complex phenomena like anode break excitation arising from gating variable interactions.